



Article

Unveiling Population Structure Dynamics of *Populus euphratica* Riparian Forests Along the Tarim River Using Terrestrial LiDAR

Alfidar Arkin ^{1,†}, Asadilla Yusup ^{2,†} , Ümüt Halik ^{1,*} , Abdulla Abliz ³, Ailiya Ainiwaer ¹, Aolei Tian ¹ and Maimaiti Mijiti ⁴

¹ College of Ecology and Environment, Ministry of Education Key Laboratory of Oasis Ecology, Xinjiang University, Urumqi 830017, China; alfidar@stu.xju.edu.cn (A.A.); eliyar641@126.com (A.A.); auto_tian@163.com (A.T.)

² Institute of Ecology, College of Urban and Environmental Sciences, Peking University, Beijing 100871, China; asadilla@pku.edu.cn

³ College of Tourism, Key Laboratory of the Sustainable Development of Xinjiang's Historical and Cultural Tourism, Xinjiang University, Urumqi 830046, China; abdulla.abliz@xju.edu.cn

⁴ School of Economics and Management, University of Chinese Academy of Sciences, Beijing 100190, China; mmtmijiti@163.com

* Correspondence: halik@xju.edu.cn

† These authors contributed equally to this work.

Abstract: The *Populus euphratica* desert riparian forest, predominantly distributed along the Tarim River in northwestern China, has experienced significant degradation due to climate change and anthropogenic activities. Despite its ecological importance, systematic assessments of *P. euphratica* stand structure across the entire Tarim River remain scarce. This study employed terrestrial laser scanning (TLS) to capture high-resolution 3D structural data from 2741 individual trees across 30 plots within six transects, covering the 1300 km mainstream of the Tarim River. ANOVA, PCA, and RDA were applied to examine tree structure variation and environmental influences. Results revealed a progressive decline in key structural parameters from the upper to lower reaches of the river, with the lower reaches showing pronounced degradation. Stand density decreased from 440 to 257 trees per hectare, mean stand height declined from 9.3 m to 5.6 m, mean crown diameter reduced from 4.1 m to 3.8 m, canopy cover dropped from 62% to 42%, and the leaf area index fell from 0.51 to 0.29. Age class distributions varied along the river, highlighting population structures indicative of growth in the upper reaches, stability in the middle reaches, and decline in the lower reaches. Abiotic factors, including groundwater depth, soil salinity, soil moisture, and precipitation, exhibited strong correlations with stand structural parameters ($p < 0.05$, $R^2 \geq 0.69$). The findings highlight significant spatial variations in tree structure, with healthier growth in the upper reaches and degradation in the lower reaches, enhance our understanding of forest development processes, and emphasize the urgent need for targeted conservation strategies. This comprehensive quantification of *P. euphratica* stand structure and its environmental drivers offer valuable insights into the dynamics of desert riparian forest ecosystems. The findings contribute to understanding forest development processes and provide a scientific basis for formulating effective conservation strategies to sustain these vital desert ecosystems, as well as for the monitoring of regional environmental changes.

Keywords: LiDAR; stand structure change; riparian forest; principal components analysis; *Populus euphratica*; Tarim River



Academic Editors: Jozef Výboštok, Arunima Singh and Juliána Chudá

Received: 4 January 2025

Revised: 14 February 2025

Accepted: 16 February 2025

Published: 18 February 2025

Citation: Arkin, A.; Yusup, A.; Halik, Ü.; Abliz, A.; Ainiwaer, A.; Tian, A.; Mijiti, M. Unveiling Population Structure Dynamics of *Populus euphratica* Riparian Forests Along the Tarim River Using Terrestrial LiDAR. *Forests* **2025**, *16*, 368. <https://doi.org/10.3390/f16020368>

Copyright: © 2025 by the authors. Licensee MDPI, Basel, Switzerland. This article is an open access article distributed under the terms and conditions of the Creative Commons Attribution (CC BY) license (<https://creativecommons.org/licenses/by/4.0/>).

1. Introduction

The Euphrates poplar (*Populus euphratica* Oliv.) is a keystone tree species in the desert riparian forests of Central Asia, particularly along the Tarim River in northwestern China [1–3]. This species plays an irreplaceable ecological role in this fragile, arid ecosystem, contributing to regional ecological stability, biodiversity conservation, soil erosion prevention, and combating desertification [4,5]. However, *P. euphratica* forests are increasingly threatened by climate change and anthropogenic pressures [6,7].

The Tarim River Basin is characterized by a temperate, continental arid desert climate. The annual precipitation ranges from 50 to 80 mm, whereas annual evaporation significantly exceeds this, reaching 2100 to 3000 mm. Seasonal temperature variations are extreme, with summer temperatures rising to 45 °C in July and winter temperatures dropping as low as −30 °C in January. The average annual temperature is approximately 10 °C [8]. The Tarim River basin has experienced significant environmental degradation due to excessive water extraction for agricultural irrigation, which has reduced river flows and degraded habitats [9]. While *P. euphratica* exhibits remarkable drought tolerance, extreme climatic events such as prolonged droughts, flooding, and pest outbreaks can diminish its resilience and disrupt ecosystem balance [10]. Particularly in the lower reaches of the Tarim River, forest area has drastically declined, shrinking from 54,000 hectares in the 1950s to merely 7000 hectares in recent decades, driven largely by dam construction and water withdrawal [11]. Field surveys indicate that approximately 60% of sampled trees in this region display varying degrees of degradation, from mild to severe [12].

Understanding plant population structure is fundamental for assessing ecological stability and regeneration capacity [13]. Key population structure components include stand structure, age class pattern, density, spatial distribution, sex ratio, and genetic diversity [14]. For forest ecosystems, evaluating population structure across life stages, such as seedlings, saplings, and mature trees, provides insights into community regeneration and long-term sustainability [15]. Population structure is shaped by a complex, intricate relationship between vegetation and the environment [16]. Metrics such as stand structure, age distribution, and density are invaluable for deciphering the mechanisms underlying population formation, development, and maintenance [17,18]. Therefore, quantifying the structural attributes of *P. euphratica* populations is vital for evaluating the growth dynamics and health of desert riparian forests along the Tarim River.

Previous research has examined various aspects of *P. euphratica* populations at the regional scale, including age distribution, structural dynamics, spatial organization, competitive interactions, and genetic structure [19–22]. However, systematic studies comparing *P. euphratica* stand structures across different environmental gradients along the entire length of the Tarim River remain limited. The selection of the Tarim River as the study area was motivated by its ecological significance, the vulnerability of its riparian forest, and the pronounced environmental gradients along its course. These characteristics make the region an ideal natural laboratory for studying the population structure and ecological dynamics of *P. euphratica*.

Terrestrial laser scanning (TLS), as an active remote sensing technology, offers unprecedented precision for assessing forest structure. By capturing detailed three-dimensional (3D) data, TLS enables millimeter-level accuracy in measuring tree attributes, outperforming traditional manual methods [23–25]. Previous studies have primarily relied on long-term NDVI-based satellite imagery to quantify the restoration dynamics of *P. euphratica* forests, with most analyses conducted at the population scale rather than the individual tree level. Moreover, these studies have not sufficiently refined the impact of ecological water conveyance on individual trees and their spatial distribution patterns [26]. Recent studies highlight TLS's capability to accurately assess vertical forest structures with a precision of

up to 93% [27,28]. Beyond individual tree assessments, TLS facilitates community-level analyses, offering detailed structural insights crucial for understanding forest dynamics [29]. Furthermore, integrating ALS (Aerial laser scanner) or UAV (Unmanned aerial vehicle) LiDAR with TLS can reduce occlusions and enhance the accuracy of structural parameter calculations. Applying this integrated methodology to time series data could provide even deeper insights into forest dynamics over time [30].

In this study, we employed TLS to investigate the population structure of *P. euphratica* under varying growth conditions along the 1300 km mainstream of the Tarim River. Six research transects were selected across the river's upper, middle, and lower reaches to acquire individual-scale tree structure data. The objectives of this study were to (1) compare the stand structural characteristics of *P. euphratica* populations across different sections of the Tarim River, (2) analyze trends in age class distribution patterns within *P. euphratica* populations across the transects, and (3) identify abiotic factors significantly associated with changes in *P. euphratica* population structure. Given the pronounced environmental gradients along the Tarim River, we hypothesize that from the upper to the lower reaches, the structural integrity of *P. euphratica* forests will exhibit a significant decline. Specifically, both individual tree and stand structural are expected to show a progressive deterioration downstream, reflecting increasing water stress, soil salinity, and habitat degradation. This research advances our understanding of the structural dynamics of *P. euphratica* forests and their responses to environmental gradients, providing valuable insights for the conservation and management of desert riparian ecosystems.

2. Methods

2.1. Study Area

This study was conducted along the main stem of the Tarim River in northwestern China (Figure 1), a region characterized by a temperate continental arid climate. Annual precipitation ranges from 50 to 80 mm, while evaporation exceeds this at 2100 to 3000 mm. Temperature variations are extreme, with summer highs reaching 45 °C in July and winter lows dropping to −30 °C in January. The average annual temperature is around 10 °C [8]. The main soil types in this area are Fluvisols, Gleysols, Solonchak, and Arenosols, which are influenced by the region's arid conditions and high salinity levels [31]. The local vegetation comprises a relatively simple community structure dominated by species adapted to extreme drought and salinity. Among these, *P. euphratica* stands out as the dominant tree species, forming the primary component of the desert riparian forest ecosystem along the Tarim River [3]. The Tarim Rivers channels vary spatially and temporally. Spatially, they differ across the river's upper, middle, and lower reaches, influenced by topography and human activities like dams. Temporally, water flow is higher in spring and summer due to snowmelt and rainfall but reduced in winter, causing drying in some lower reaches. This unique forest ecosystem provides critical ecological services in an otherwise harsh environment, making it an essential subject for restoration and conservation efforts [4]. The selection of the Tarim River as the study area was motivated by its ecological significance, the vulnerability of its riparian forest, and the pronounced environmental gradients along its course. These characteristics make the region an ideal natural laboratory for studying the population structure and ecological dynamics of *P. euphratica*.

Additionally, remote sensing techniques and GIS-based analyses have been widely used in assessing riparian forests, providing valuable insights into vegetation dynamics and environmental changes [32,33]. The selection of the Tarim River as the study area was motivated by its ecological significance, the vulnerability of its riparian forest, and the pronounced environmental gradients along its course. These characteristics make the

region an ideal natural laboratory for studying the population structure and ecological dynamics of *P. euphratica*.

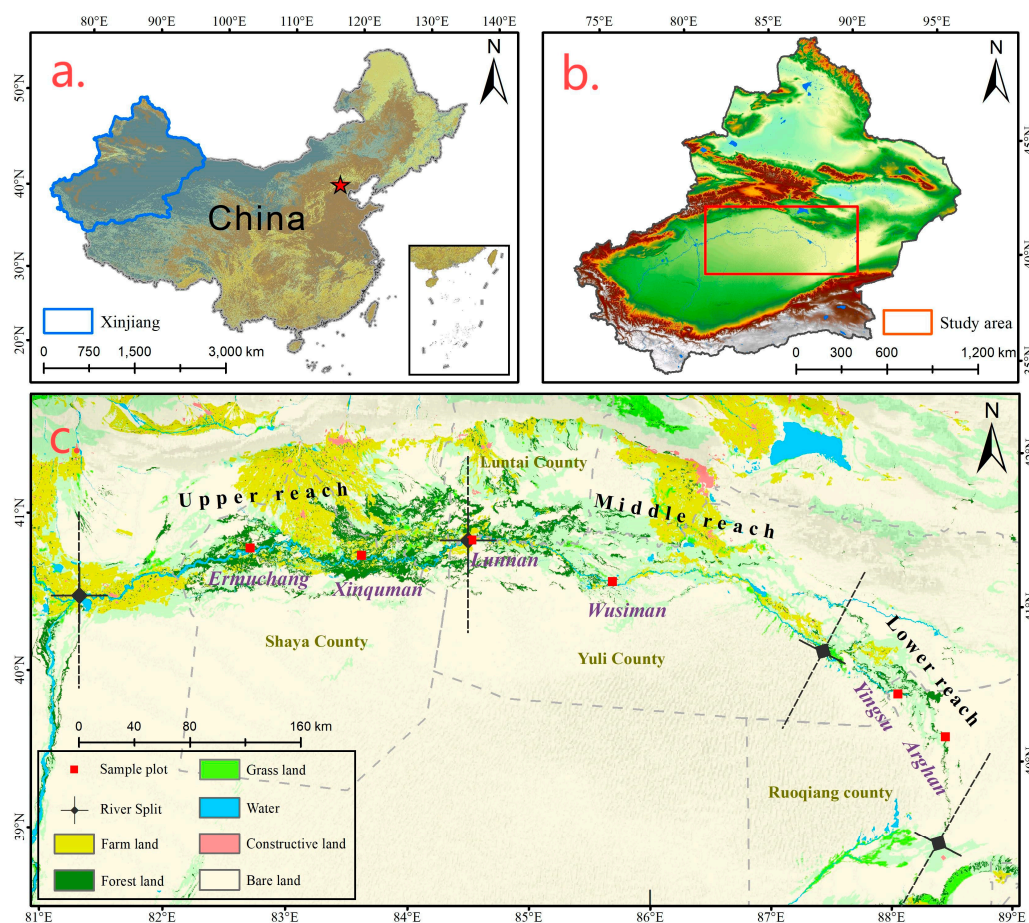


Figure 1. Sketch map of research transects along the main stream of the Tarim River. Note: (a) Map of China, (b) presents the topography of Xinjiang, with the study area clearly defined by the red rectangular box, (c) presents a detailed map of the study area, covering information on land use types, river distribution, and sampling site locations within the region.

2.2. Sample Plot Setting

Six research transects were selected along the upper, middle, and lower reaches of the Tarim River to represent different environmental gradients (Table 1). These transects were located at Ermuchang, Xinquman, Lunnan, Wusiman, Yingsu, and Arghan (Figure 1). Each transect encompassed five plots established within a 1 km range from the river channel, with a consistent spacing of 200 m between adjacent plots to ensure comprehensive spatial coverage and minimize sampling bias. Each plot is a square area with a side length of 50 m. Plots were labeled as A1, B1, C1, D1, E1, and F1, with those closest to the river channel positioned to capture the influence of proximity to water on *P. euphratica* forest structure. This design enabled a systematic comparison of forest population attributes across the different transects. A total of 30 plots were surveyed using TLS to acquire detailed 3D structural data of individual trees. This approach ensured precise and consistent measurements of stand parameters under varying environmental conditions along the Tarim River. The chosen plot layout and spacing facilitated the analysis of spatial heterogeneity and environmental influences on *P. euphratica* population structure.

Table 1. Information of surveyed plots along the main stream of the Tarim River.

Transects	Location	Number of Plots	Plots ID	Center Longitude	Center Latitude
Upper reaches	Ermuchang (Shaya County)	5	A1–A5	82°21′49.42″ E	40°57′47.86″ N
	Xinquman (Shaya County)	5	B1–B5	83°18′36.04″ E	40°59′54.55″ N
Middle reaches	Lunnan (Luntai County)	5	C1–C5	85°27′39.34″ E	40°59′31.99″ N
	Wusiman (Luntai County)	5	D1–D5	84°13′57.69″ E	41°10′27.52″ N
Lower reaches	Yingsu (Yuli County)	5	E1–E5	87°57′13.02″ E	40°23′48.53″ N
	Arghan (Ruoqiang County)	5	F1–F5	88°22′25.63″ E	40°08′09.81″ N

Note: All data were collected during the period from June to August 2024.

2.3. TLS Data Pre-Processing

The TLS data were acquired with a RIEGL VZ-1000 TLS (Riegl, Co., Ltd., Salzburg, Austria) from five diametrically arranged positions in each plot, with a scanning accuracy of ± 5 mm/100 m, depending on the micro-topography and stand density conditions of the selected sample areas. The data were collected using the fine scanning mode, with a scanning time of 15 min per station. The overlap between adjacent stations was greater than 70%, and the scanning distance was set to 450 m. The multi-station point cloud data were aligned into a unified coordinate system using RiSCAN Pro v2.7 (Riegl, Co., Ltd., Salzburg, Austria) with a mean standard deviation of 0.01 m. The number of trees, tree height (H), calculated as the height difference between the highest point (Zmax) and the ground point (Zmin) from segmented point cloud data, diameter at breast height (DBH) extracted from point clouds between 1.25 and 1.35 m above the ground and determined using Hough transformation for circle fitting, and crown diameter (CD) calculated as the average of the longest and shortest distances relative to the crown area were determined for each plot using the commercial software package LiDAR 360 v4.0 (Beijing Green Valley Technology Co., Ltd., Beijing, China). Despite the high precision of TLS measurements, occlusions occasionally impeded data acquisition, particularly for DBH, where 88.9% of tree trunks were successfully measured. Occlusions were primarily caused by overlapping canopies and obstructed views of tree bases, which limited the completeness of the TLS scans (Figure 2).

2.4. Age Classification and Calculation of Stand Structural Parameters

All measured trees were classified into five distinct age classes based on their DBH, following the classification criteria established by Wang [1]. The age classes were defined as seedlings ($DBH \leq 5$ cm), young trees ($5 \text{ cm} < DBH \leq 15$ cm), near-mature trees ($15 \text{ cm} < DBH \leq 30$ cm), mature trees ($30 \text{ cm} < DBH \leq 50$ cm), and over-mature trees ($DBH > 50$ cm). This classification facilitated the assessment of population dynamics across various developmental stages, aiding in the evaluation of regeneration potential and the overall health of *P. euphratica* stands along the Tarim River.

Stand structural parameters were derived from individual tree attributes obtained from the TLS data to characterize the population structure of *P. euphratica* stands. Stand density was determined by calculating the number of trees per unit area ($n \cdot \text{ha}^{-1}$). Canopy cover was quantified as the proportion of the area covered by the canopy. The gap fraction, representing the presence of gaps in the forest canopy due to the death of dominant tree species during the mature stage of a forest stand [34], was calculated as the proportion of normalized ground points to the total point cloud. The leaf area index was estimated by integrating the leaf area density over the height of the canopy. These parameters provide a comprehensive understanding of the structural characteristics and ecological dynamics of *P. euphratica* populations along the Tarim River.

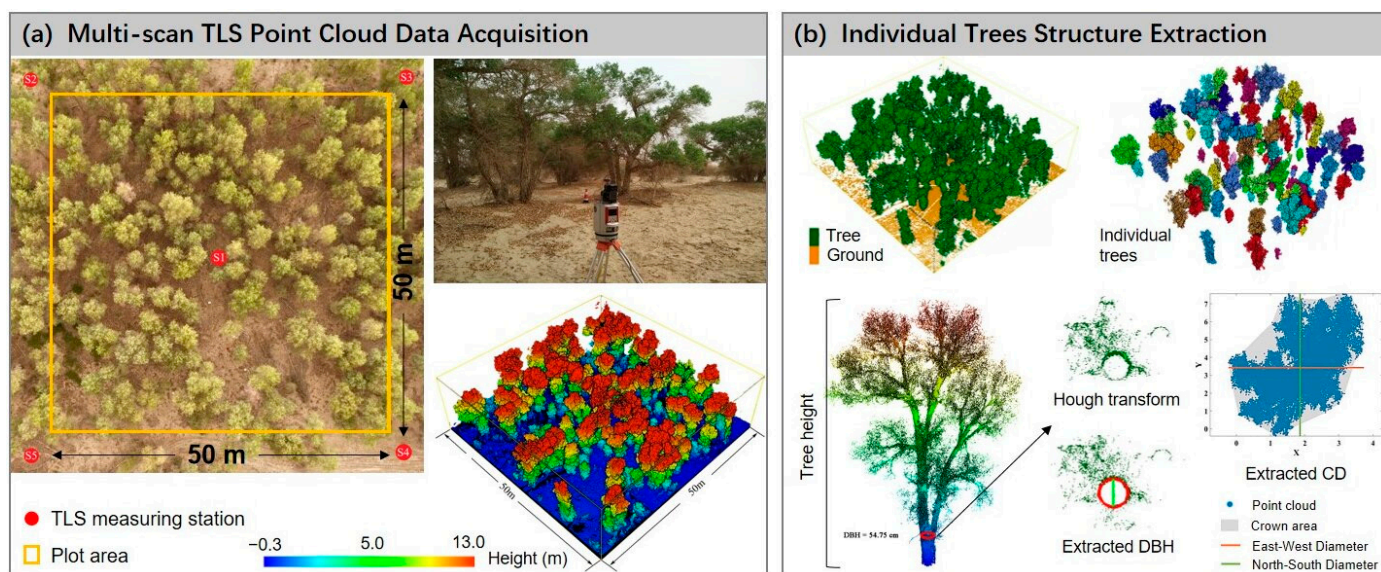


Figure 2. Extraction of tree structural attributes using TLS point cloud. Note: (a) TLS data acquisition in the sample plot (50 × 50 m); raw data. (b) The classification of tree and ground point clouds, segmentation of individual trees, and measurement of tree height (H), crown diameter (CD), and diameter at breast height (DBH) are all performed using the point cloud data.

2.5. Acquisition of Abiotic Factors

To analyze the influence of abiotic factors on the structural characteristics of *P. euphratica* stands, data on soil properties, groundwater depth, and climatic conditions were collected. Soil moisture, salinity, and pH were measured at depths of 30 cm, 60 cm, and 90 cm within each plot using the Hydra Soil Detection Sensor (Stevens, Co., Ltd., Horn, Germany) to assess the electrical conductivity of the soil solution, which is indicative of its salt content, while soil organic matter content was quantified using the potassium dichromate volumetric method to assess soil fertility and carbon storage. Groundwater depth data were obtained from monitoring wells established by the Tarim River Basin Management Bureau at each transect. Additionally, annual precipitation data representing climatic variables were sourced from the regional statistical yearbook.

To determine the relationships between stand structural parameters (e.g., stand density, canopy cover) and abiotic factors (e.g., soil moisture, salinity, groundwater depth), Pearson correlation analysis was performed. This analysis evaluated the linear associations between different variables [35]. ANOVA was conducted using MATLAB (<https://www.mathworks.com/products/matlab.html>) to compare tree structural parameters (e.g., tree height, diameter at breast height, and crown diameter) across different regions (upper, middle, and lower reaches) of the Tarim River. The results of ANOVA indicated significant differences in tree structure between the regions, with p -values < 0.05, suggesting that the environmental conditions influence forest structure. Further, both principal component analysis (PCA) and redundancy analysis (RDA) were performed using CANOCO v5.0 (Microcomputer Power Co., Ltd., Ithaca, NY, USA) to examine the combined effects of abiotic factors on stand structure. PCA was used to visualize the variance in tree structure and environmental gradients, while RDA assessed how environmental variables explain the variation in stand structure [36]. In the RDA results, the length of each arrow represented the strength of the relationship between variables and the two main ordination axes, while the orientation indicated the direction of correlations. Variables pointing in the same direction were positively correlated, whereas those pointing in opposite directions were negatively correlated. This integrative analysis provided comprehensive insights into the environmental drivers shaping *P. euphratica* population structure along the Tarim River.

3. Results

3.1. Tree Structural Characteristics Along Different Transects of the Tarim River

A total of 2741 individual *P. euphratica* trees were measured using TLS across all sampling plots, with variations in stand characteristics observed along the upper, middle, and lower reaches of the Tarim River (Table 2). The number of trees recorded in the upper, middle, and lower reaches was 1101, 998, and 642, respectively, indicating a decreasing trend in tree abundance downstream. Correspondingly, the mean stand densities were 440, 399, and 257 trees per hectare in the upper, middle, and lower reaches, respectively.

Table 2. Number of individual trees acquired by TLS in each plot.

Upper Reaches			Middle Reaches			Lower Reaches		
Plot ID	Number of Tree	Stand Density (n·ha ⁻¹)	Plot ID	Number of Tree	Stand Density (n·ha ⁻¹)	Plot ID	Number of Tree	Stand Density (n·ha ⁻¹)
A1	258	1032	C1	92	368	E1	84	336
A2	103	412	C2	131	524	E2	56	224
A3	127	508	C3	127	508	E3	82	328
A4	104	416	C4	85	340	E4	48	192
A5	101	404	C5	99	396	E5	23	92
B1	117	468	D1	151	604	F1	99	396
B2	94	376	D2	106	424	F2	72	288
B3	107	428	D3	69	276	F3	74	296
B4	91	364	D4	78	312	F4	66	264
B5	59	236	D5	61	244	F5	39	156
Total	1101	440	Total	998	399	Total	642	257
Interval	(78, 154)	(312, 616)	Interval	(79, 120)	(316, 482)	Interval	(47, 80)	(191, 322)

In the upper reaches, plots A1, A3, and B1 exhibited the highest tree counts, suggesting favorable growth conditions in these areas. Similarly, in the middle reaches, plots C2, C3, and D1 showed the highest tree counts, while plots E1 and F1 dominated in the lower reaches. Across all transects, plots located closer to the river channel (e.g., A1, B1, C2, D1, E1, F1) consistently displayed the highest tree densities, highlighting the importance of proximity to water in sustaining tree populations. In contrast, plots situated farther from the river channel (e.g., B4, B5, C4, C5, D3, D4, D5, E4, E5, F4, F5) recorded significantly lower tree counts, indicating a decline in tree density with increasing distance from the water source.

Notably, the tree counts in most plots within the lower reaches were markedly lower compared to those in the upper and middle reaches. This pattern reflects the cumulative impacts of environmental stressors, such as reduced water availability and salinity, on forest structure downstream. These findings underscore the spatial heterogeneity in *P. euphratica* stand characteristics and highlight the critical role of water availability in shaping tree population dynamics along the river. The distribution of H, DBH, and CD for all measured *P. euphratica* trees across the three transects generally followed a normal distribution pattern, although the value ranges differed significantly between reaches (Figure 3). In the upper reaches, the distribution of tree height showed considerable variability, with a maximum height of 19.9 m, indicating a broad spectrum of tree sizes (Figure 3a). The middle reaches also exhibited a wide range of tree heights, with a maximum height of 17.2 m (Figure 3b). Conversely, the lower reaches displayed a narrower distribution of tree heights, with a maximum of 10.6 m, suggesting a more uniform but shorter tree structure in these areas (Figure 3c). The mean tree height across the upper, middle, and lower reaches was 9.3 m, 8.9 m, and 5.6 m, respectively, reflecting a clear decline in tree height as one moves

downstream. The distribution of DBH in the upper reaches was markedly skewed towards smaller values, with a maximum DBH of 99.61 cm, indicating a dominance of smaller trees in this transect (Figure 3d). In the middle reaches, DBH distribution showed a concentration of both small- and medium-sized trees, with a maximum DBH of 102.72 cm (Figure 3e). The lower reaches exhibited a more even distribution, with fewer trees at both small and large DBH values and a maximum DBH of 88.10 cm, which suggests potential growth constraints in this region (Figure 3f). The mean DBH was highest in the middle reaches (26.86 cm), followed by the lower reaches (25.23 cm) and the upper reaches (21.8 cm), suggesting a trend of larger trees in the middle section of the river. The CD distribution followed a similar trend to that of tree height, with the upper and middle reaches displaying relatively wide ranges. The maximum CD in the upper reaches was 13.63 m, while in the middle reaches, it reached 13.72 m (Figure 3g,h). In contrast, the lower reaches showed a narrower CD distribution, with a maximum value of 9.74 m (Figure 3i). Overall, both tree height and CD exhibited a decreasing trend from the upper to the lower reaches, particularly in the lower reaches. In contrast, DBH increased progressively from the upper to lower reaches. These patterns highlight the structural differences in *P. euphratica* stands along the river, with larger and more diverse trees in the upper and middle reaches compared to the more constrained growth observed in the lower reaches.

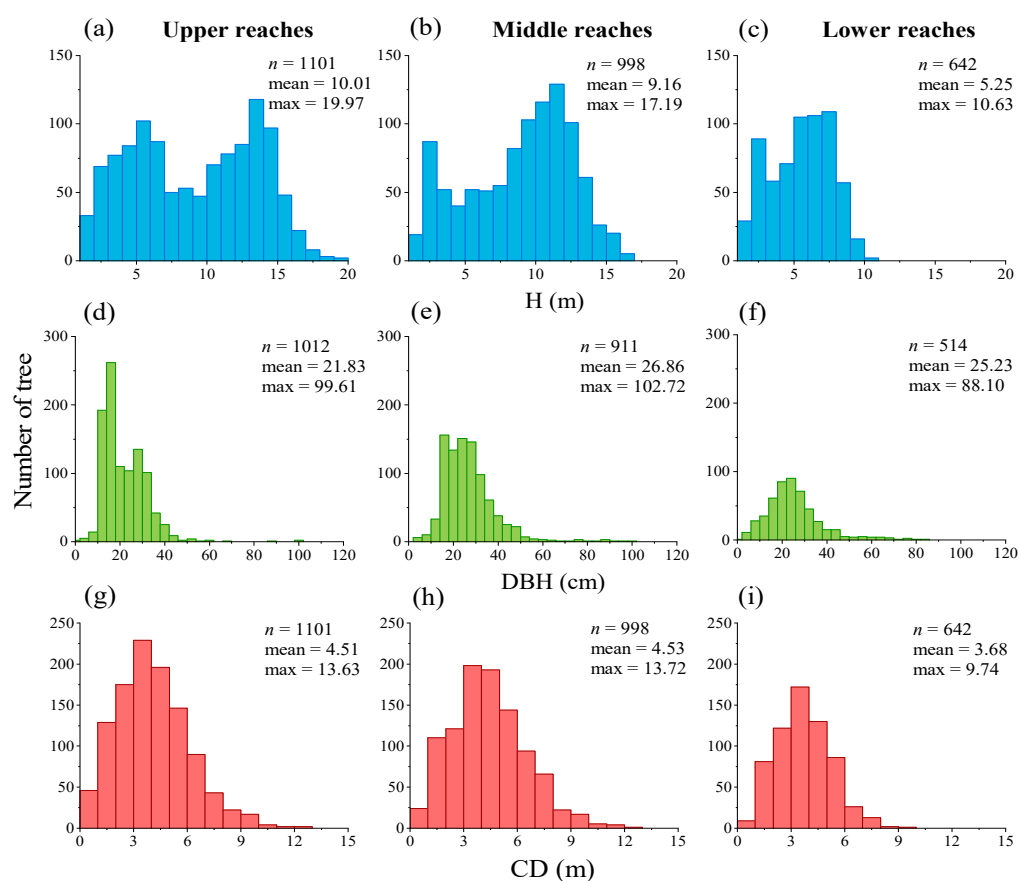


Figure 3. Distribution patterns of *P. euphratica* tree structural attributes (H, DBH, and CD) in the upper, middle, and lower reaches of the Tarim River. Note: (a–c) show the distribution of tree height (H); (d–f) show the distribution of diameter at breast height (DBH); (g–i) show the distribution of crown diameter (CD). The number of trees counted in (d–f) is relatively smaller because the TLS was unable to obtain the DBH of a few trees.

The ANOVA results indicate significant differences in *P. euphratica* structural attributes (H, DBH, and CD) across the upper, middle, and lower reaches of the Tarim River (Figure 4). The F-values (245.01 for H, 39.09 for DBH, and 25.92 for CD) suggest that the between-group variance substantially exceeds the within-group variance, confirming a notable spatial variation in forest structure. The p -values (all <0.001) indicate that these differences are statistically significant. Specifically, tree height, DBH, and crown diameter exhibit a progressive decline downstream, supporting the hypothesis that *P. euphratica* stands experience structural deterioration along the river's course. This trend is likely driven by increasing water stress, soil salinity, and habitat degradation in the lower reaches. The significant F-values and low p -values confirm that the structural decline is not random but systematically associated with environmental gradients, reinforcing the impact of hydrological and edaphic conditions on forest integrity.

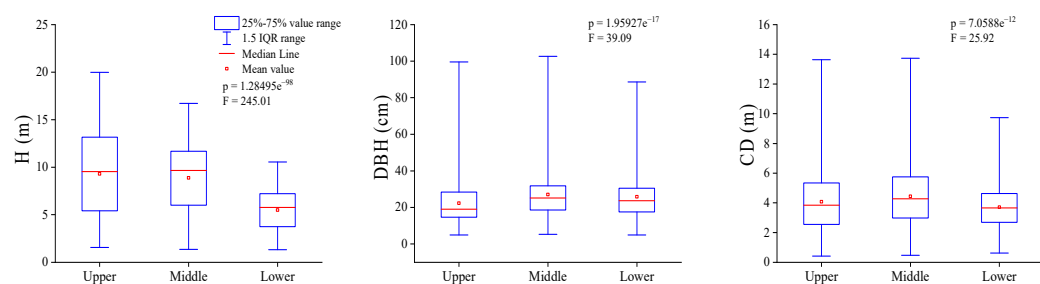


Figure 4. Comparison of *P. euphratica* tree structural attributes (H, DBH, and CD) across the upper, middle, and lower reaches of the Tarim River.

3.2. Stand Structure Characteristics Along Different Transects of the Tarim River

Significant variations in stand structure were observed across the upper, middle, and lower reaches of the Tarim River (Table 3). In the upper reaches, stand mean H ranged from 4.88 to 12.64 m, with the majority of plots exhibiting stand mean H between 9 and 11 m, suggesting favorable conditions for tree growth. The middle reaches showed a stand mean H ranging from 6.76 to 10.56 m, with most plots having a consistent mean H between 8 and 10 m, indicating relatively stable growth conditions. In contrast, the lower reaches exhibited generally lower stand mean H, ranging from 4.17 to 6.76 m, which reflects limited vertical growth, possibly due to less favorable environmental conditions or other constraints.

In terms of stand mean DBH, lower values were recorded in plots closest to the river (A1, B1, D1, E1, F1), which may reflect a concentration of younger or smaller trees in these areas. Conversely, plots located farther from the river exhibited larger DBH values, suggesting older or more mature trees in these regions (Table 3). Canopy cover and leaf area index were highest in plots situated between 200 and 600 m from the river, indicating optimal growing conditions at these intermediate distances from the river channel.

The stand mean gap fraction, which represents the proportion of the canopy cover absent of trees, was notably higher in the lower reaches compared to the upper and middle reaches. This suggests a higher degree of canopy openness and potentially greater tree mortality or other disturbances in the lower reaches (Table 3). These variations in stand structure across the transects highlight the influence of distance from the river and other environmental factors on the growth and composition of *P. euphratica* forests along the Tarim River.

Table 3. Stand structure characteristics of *P. euphratica* in different transect plots.

Transects	Plots ID	Mean H (m)	Mean DBH (cm)	Mean CD (m)	Leaf Area Index	Canopy Cover (%)	Gap Fraction (%)
Upper reaches	A1	4.88	14.43	2.46	0.21	47	38
	A2	10.22	22.85	4.46	1.02	89	3
	A3	9.59	22.81	4.34	0.60	70	21
	A4	12.64	31.42	5.26	0.66	72	22
	A5	10.37	24.71	5.63	0.69	66	24
	B1	9.53	20.94	4.86	0.36	56	27
	B2	11.22	24.03	4.81	0.32	53	25
	B3	10.78	23.44	3.99	0.28	49	38
	B4	11.73	27.06	3.98	0.28	46	34
	B5	9.16	38.96	5.40	0.66	69	29
Middle reaches	C1	10.56	27.97	4.57	0.64	63	37
	C2	8.35	26.56	4.06	0.57	71	28
	C3	9.09	24.89	4.84	0.61	68	26
	C4	9.54	29.12	4.48	0.47	58	42
	C5	8.93	31.71	4.67	0.50	66	26
	D1	6.76	21.88	3.62	0.34	42	59
	D2	8.35	23.59	4.03	0.41	56	40
	D3	9.94	26.16	4.83	0.29	53	36
	D4	10.41	26.95	4.56	0.38	55	34
	D5	9.72	37.52	5.56	0.29	45	55
Lower reaches	E1	5.40	30.69	4.24	0.40	57	35
	E2	5.12	24.17	3.60	0.34	39	56
	E3	5.40	20.06	3.28	0.32	43	48
	E4	4.18	24.49	3.02	0.19	32	67
	E5	4.17	26.51	3.34	0.30	37	69
	F1	6.27	22.21	3.53	0.32	51	57
	F2	6.76	25.64	4.39	0.33	49	53
	F3	5.77	22.99	3.86	0.25	40	59
	F4	5.03	25.16	3.36	0.25	39	64
	F5	4.42	38.11	4.25	0.17	29	70

3.3. Age Class Distribution Changes of *P. euphratica* Along the Different River Transects

The age class distribution pattern of *P. euphratica* varied significantly across the different transects of the Tarim River, reflecting distinct growth patterns and stages of tree development along the river's course.

In the upper reaches, the tree population was characterized by a relatively high proportion of seedlings and near-mature trees, with near-mature individuals making up approximately 45% of the total population (Figure 5). This suggests that the upper reaches support a vigorous tree population, with a significant portion of trees approaching maturity. In the middle reaches, the near-mature age class dominated the distribution, comprising 58% of the tree population, indicating that the majority of trees were in a rapid growth phase. In contrast, the proportions of seedlings and young trees were relatively low, at 5% and 8%, respectively (Figure 5). This distribution suggests that the middle reaches are in a stage of sustained growth, with fewer young trees entering the population compared to the upper reaches. In the lower reaches, higher proportions of trees were found in the mature and over-mature stages, accounting for 31% and 9%, respectively. This indicates an older tree population, with fewer younger individuals present. The higher representation of mature and over-mature trees in the lower reaches suggests a shift towards a more senescent forest structure, likely due to slower growth rates and possibly environmental stressors. These age class distribution patterns highlight the varying growth dynamics of *P.*

euphratica across different sections of the river, reflecting both ecological conditions and the life cycle stages of the trees in each region.

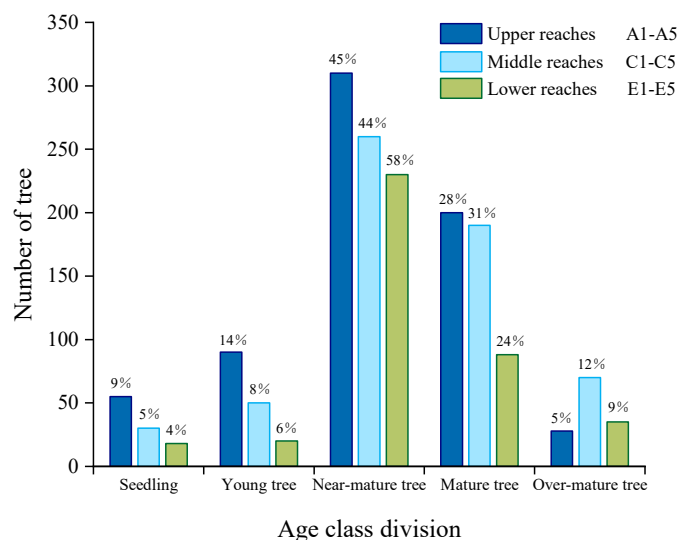


Figure 5. Age class distribution of *P. euphratica* across the upper, middle, and lower reaches of the Tarim River.

3.4. Correlation Between *P. euphratica* Stand Structural Attributes and Abiotic Factors Across Different Transects

The relationship between *P. euphratica* stand structural attributes and abiotic factors across the different river transects revealed significant correlations that highlight the influence of environmental variables on tree growth and stand characteristics. Groundwater depth exhibited a significant negative correlation ($p < 0.05$) with tree height (H), stand density, and the number of seedling trees. Additionally, groundwater depth was moderately negatively correlated with the number of young, near-mature, and mature trees, as well as with canopy cover (Figure 6). These results suggest that lower groundwater levels may limit tree growth and reduce the establishment of seedlings and younger trees. Soil moisture showed a positive correlation ($p < 0.05$) with H, stand density, canopy cover, leaf area index, the number of mature trees, and the overall tree count. This indicates that higher soil moisture availability supports better tree growth, higher stand density, and greater canopy development. On the other hand, soil salinity exhibited a negative correlation ($p < 0.05$) with most growth-related parameters, including H and CD, suggesting that higher soil salinity levels may hinder tree growth and structural development. Soil organic matter content and pH values were not significantly correlated with tree structural parameters, indicating that these factors may have a lesser impact on tree growth in the study area compared to other abiotic factors. Lastly, annual precipitation showed a positive correlation ($p < 0.05$) with the total number of trees, highlighting the importance of precipitation in sustaining tree populations and promoting forest regeneration.

The redundancy analysis (RDA) plot provides an insightful visualization of the relationships and common patterns of change between stand structural factors and abiotic variables. The analysis reveals that the first axis (Axis-1) accounts for 67.26% of the variation, while the second axis (Axis-2) explains 18.43%, together accounting for 85.69% of the total variance (Figure 7). This indicates that the factors aligned closely with Axis-1 are particularly influential in shaping the structural characteristics of *P. euphratica* stands.

The redundancy analysis (RDA) and principal components analysis (PCA) plot provide an insightful visualization of the relationships and common patterns of change between stand structural factors and abiotic variables. Combined with PCA results, it further

confirms that hydrological factors and precipitation play a dominant role in shaping stand structure. The analysis reveals that the first axis (Axis-1) accounts for 67.26% of the variation, while the second axis (Axis-2) explains 18.43%, together accounting for 85.69% of the total variance (Figure 7). This indicates that the factors aligned closely with Axis-1 are particularly influential in shaping the structural characteristics of *P. euphratica* stands.

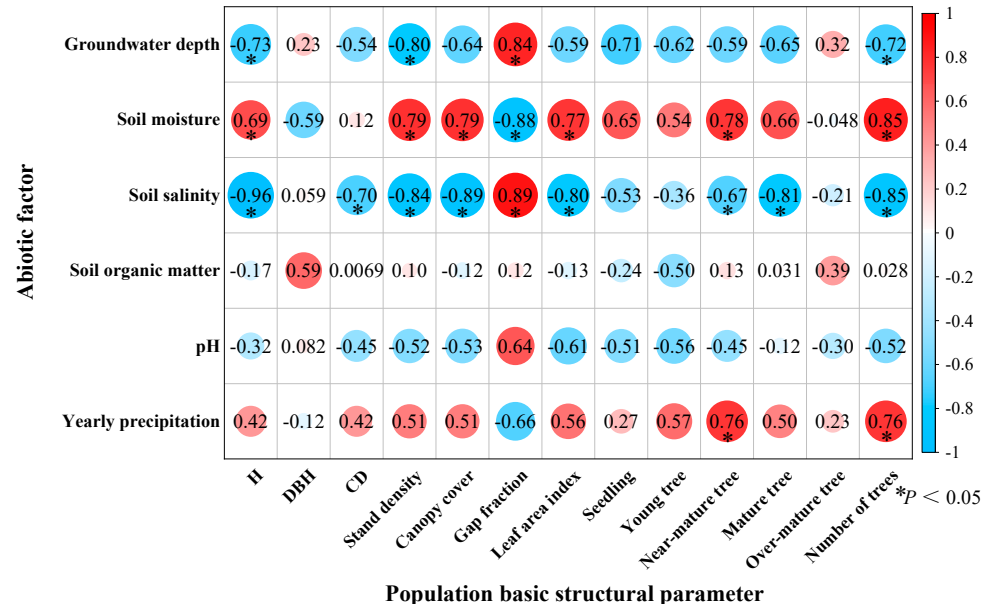


Figure 6. Correlation between *P. euphratica* basic structural parameters and abiotic factors.

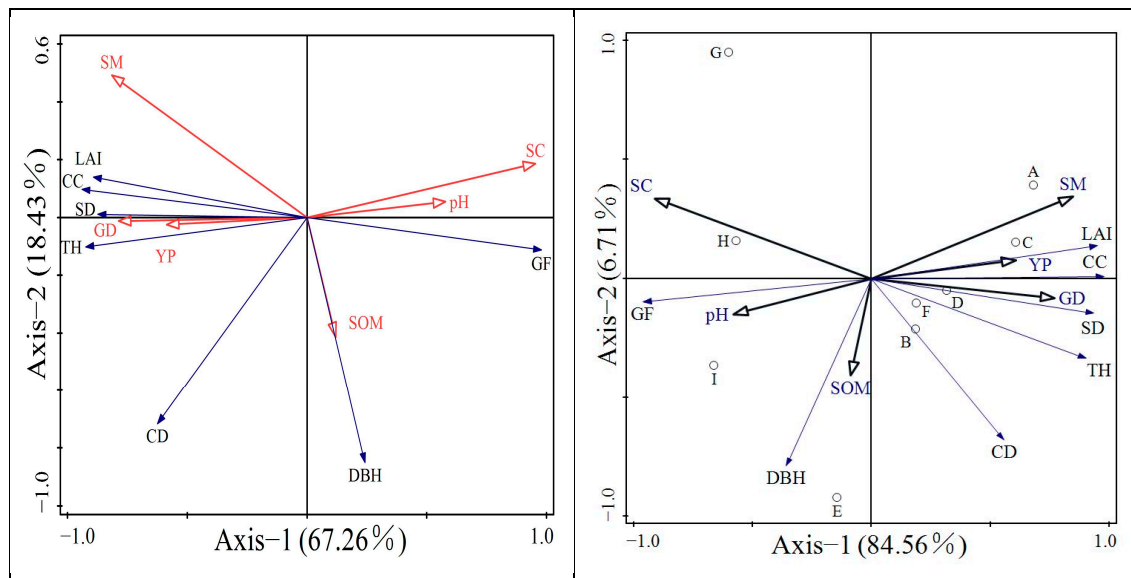


Figure 7. Redundancy analysis and principal components analysis of *P. euphratica* stand structures and abiotic factors. Note: Arrows denote variable directions or vectors. Lengths and directions show contributions to principal components: longer means more influence, shorter less. Directions indicate variable orientation in the space. Different letters (A–I) with small circles are different sample points. Observing their distribution analyzes sample similarities/differences. Clustered circles suggest similar features, dispersed ones imply differences. This pattern reveals potential data structures or grouping info.

Stand mean H, stand density, canopy cover, and leaf area index clustered together along the positive direction of Axis-1, demonstrating strong positive correlations with yearly precipitation. This suggests that higher precipitation levels facilitate greater canopy

development, tree growth, and higher stand density. In contrast, groundwater depth, soil moisture, and soil salinity were oriented along the negative side of Axis-1, indicating a negative association with growth-related attributes such as DBH, CD, and canopy cover. These factors appear to limit tree growth, as higher groundwater depth, lower soil moisture, and increased soil salinity are associated with reduced tree size and structural development. This pattern underscores the significant role of precipitation in promoting healthy tree growth, while groundwater depth, soil moisture, and salinity are key limiting factors that negatively affect the structural characteristics of *P. euphratica* stands. The interplay between these variables, as highlighted by both RDA and PCA, suggests that effective water management is crucial for sustaining *P. euphratica* populations under changing environmental conditions.

To assess the impact of groundwater depth on tree structure, we compared H, DBH, and CD along increasing distances from the river channel (Figure 8). In the upper and middle reaches, H generally increases with distance, while in the lower reaches, H peaks at 200 m before declining further. DBH consistently increases across all transects, mainly due to fewer young trees. However, the CD shows no significant variation with distance.

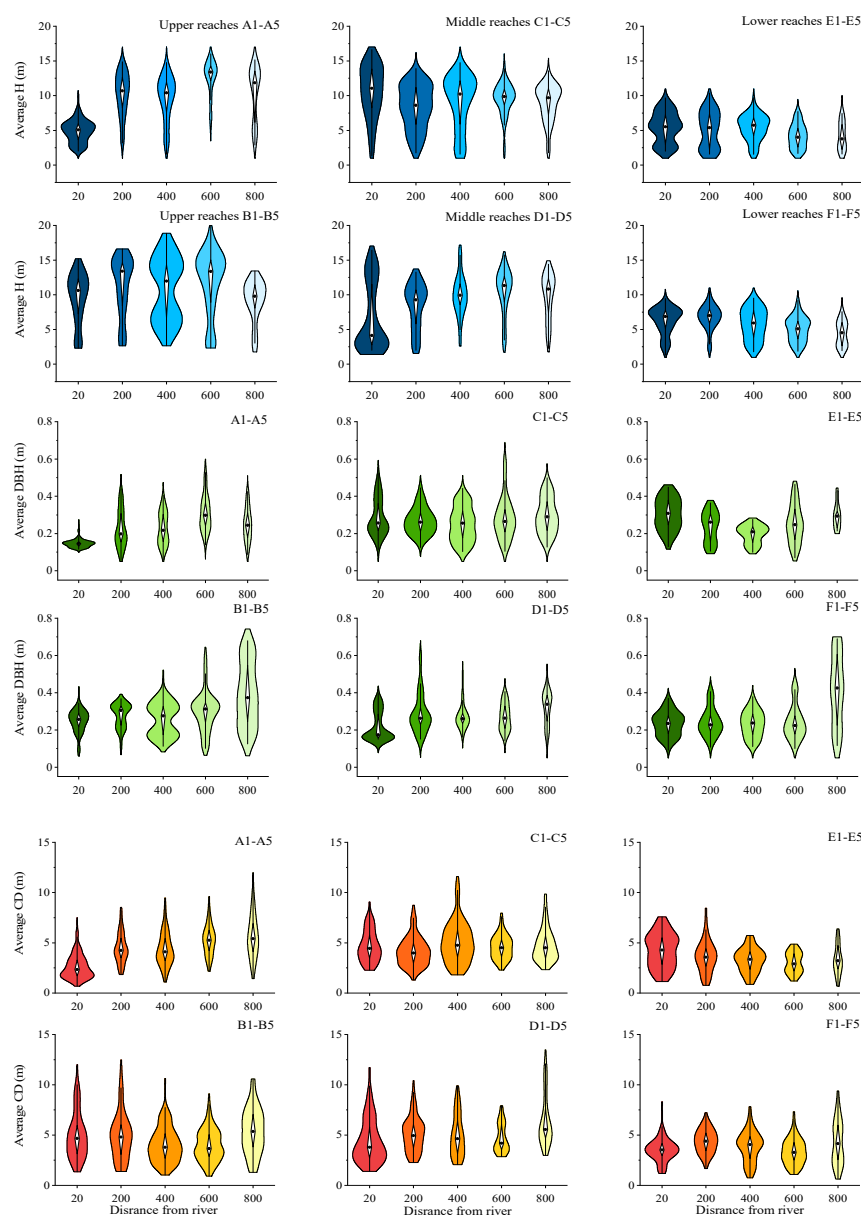


Figure 8. Response of *P. euphratica* structural parameters to increasing distance from the river channel.

4. Discussion

4.1. Change Trends in Tree and Stand Structural Parameters Along the Tarim River

The observed decline in tree density from the upper to the lower reaches of the Tarim River highlights a gradient of environmental stressors that influence tree survival and density (Table 2). This trend underscores the adaptability of *P. euphratica* to varying environmental conditions across the river system. Notably, significant variation in tree numbers within each transect suggests that local environmental factors can significantly affect tree density, even within similar river sections. Previous studies have emphasized the ability of *P. euphratica* to adapt to different habitats, with local conditions influencing stand structure [37,38].

In terms of structural dimensions, our findings align with prior research indicating that *P. euphratica* can achieve a maximum DBH of up to 120 cm and a height of approximately 15 m under optimal conditions [39]. In the upper reaches, trees generally exhibit taller heights, larger crown diameters, and higher canopy cover compared to those in the middle and lower reaches (Figure 3). These characteristics suggest that the upper reaches provide favorable conditions for tree growth, as also reported by Han et al. [40], who found that *P. euphratica* forests in these areas maintain high vitality. Conversely, trees in the lower reaches display smaller sizes, lower canopy density, and higher gap fractions, indicating degradation in stand conditions. These findings highlight the impact of spatially variable environmental factors on the structural diversity of *P. euphratica* populations across the river system.

Recent advancements in remote sensing technologies, particularly TLS, offer new possibilities for assessing these structural variations with higher accuracy. While TLS has been widely used in forest monitoring, its application in desert riparian forests remains relatively limited. Traditional field surveys often rely on labor-intensive measurements, which can be less precise and spatially constrained. In contrast, TLS provides high-resolution three-dimensional point cloud data, allowing for detailed quantification of tree height, canopy structure, and spatial distribution. In this study, TLS was deployed across multiple regions along the Tarim River, enabling a refined assessment of stand structure and density. The successful application of TLS in this study suggests its potential as a valuable tool for long-term monitoring and management of desert riparian forests, providing insights that were previously unattainable with conventional methods.

4.2. Stand Age Class Distribution Characteristics Along Different River Transects

The age class distribution across the different reaches of the river reveals distinct trends in population growth (Figure 5). In the upper reaches, the balanced structure of the population, with a substantial proportion of young and near-mature trees, suggests ongoing regeneration and stable forest dynamics. This pattern aligns with the findings of Han et al. [40], who noted that the *P. euphratica* population in the upper reaches of the Tarim River remains relatively stable despite high sapling mortality rates.

In contrast, the middle reaches exhibit a similar age class distribution but with a lower proportion of seedlings and young trees, which raises concerns about future regeneration. Xu et al. [41] and Han et al. [40] found a similar trend, where the middle reaches exhibited a normal distribution pattern with fewer young trees compared to mature ones. The lower reaches, however, display an aging population with high proportions of mature and over-mature trees and limited regeneration potential. This aligns with previous research by Wu et al. [42], who highlighted the high mortality rates of young trees in the lower reaches, leading to a lack of younger age classes and an overrepresentation of mature and over-mature individuals [43]. These findings underscore the need for conservation and management strategies that support regeneration, particularly in the middle and lower

reaches, by addressing environmental stressors such as water availability and soil salinity, which could hinder the growth of seedlings and young trees.

4.3. Response of Stand Structure to Abiotic Factors

The correlation analysis between *P. euphratica* stand structure and various abiotic factors reveals that groundwater depth and soil salinity significantly affect tree growth and stand density. Specifically, deeper groundwater levels and higher soil salinity are associated with reduced tree growth and canopy cover (Figure 6). These results are consistent with previous studies that have shown that groundwater depth plays a pivotal role in *P. euphratica* distribution, with a decrease in tree growth and stand density as groundwater depth increases [7]. Additionally, soil salinity has been shown to negatively influence regeneration success, although *P. euphratica* can tolerate moderate salinity levels if groundwater is sufficiently available [5]. Our findings support these conclusions, emphasizing that while *P. euphratica* can survive in saline conditions, excessive salinity and groundwater depletion limit its growth potential.

Similar hydrological constraints have been observed in other riparian forest ecosystems worldwide. For example, in North America, *Populus deltoides* (Cotton wood) forests rely on a stable groundwater supply and groundwater depletion has been shown to significantly reduce tree growth and increase mortality rates. Likewise, studies in the Murray–Darling Basin, Australia, have reported that declining groundwater tables lead to reduced vegetation vitality in riparian woodlands [44]. These global findings further reinforce the conclusion that hydrological conditions play a crucial role in shaping riparian forest dynamics.

Precipitation, on the other hand, plays a positive role in promoting tree growth, canopy cover, and overall stand density (Figure 7). This finding aligns with studies that emphasize the importance of water availability in the growth and vitality of *P. euphratica*. As highlighted by Ling et al. [45] and Chen et al. [46], river runoff is primarily transferred to groundwater, which supports the ecological needs of vegetation, including *P. euphratica*. The positive correlation between precipitation and tree growth observed in our study highlights the critical role of rainfall in sustaining *P. euphratica* populations, particularly in the face of climatic variability.

Additionally, *P. euphratica* exhibits remarkable adaptability to extreme drought conditions by altering its morphological characteristics. For instance, under severe drought stress, the tree reduces crown size and height, effectively optimizing resource allocation for survival [12,21]. These morphological adjustments allow the trees to endure arid conditions by sacrificing height growth and canopy size as a trade-off for survival. Such adaptive strategies are consistent with findings from Xu et al. [42] and Li et al. [47], who noted that *P. euphratica* can maintain survival in increasingly dry environments by modifying its assimilative organs. These findings emphasize the vulnerability of *P. euphratica* to changes in hydrological conditions, particularly in arid and semi-arid regions where water availability is a limiting factor. The results suggest that precipitation is a key determinant of stand structure, highlighting the potential impacts of climate change on forest dynamics. Furthermore, the ability of *P. euphratica* to adapt morphologically to drought conditions suggests that while the species can persist in harsh environments, these adaptations may compromise long-term population sustainability if environmental stressors persist.

4.4. Implications for Conservation and Management

Our findings underline the importance of groundwater and soil moisture for maintaining the structural integrity and vitality of *P. euphratica* forests. Given the critical role of these abiotic factors in shaping tree growth, conservation strategies must prioritize the protection

and restoration of hydrological conditions, including groundwater levels and soil moisture. Management efforts should also focus on mitigating the impacts of soil salinity and improving water availability, particularly in the middle and lower reaches, to support regeneration and prevent further degradation. Additionally, integrating ground-based LiDAR data with satellite LiDAR and high-resolution imagery could enhance the large-scale inversion of population structure parameters for *P. euphratica*.

Globally, water resource management has been recognized as a key strategy for riparian forest restoration. Using the Ejina Oasis as a case study, remote sensing data from 2000 to 2020 indicated increased runoff, rising groundwater levels, expanded surface water, and enhanced NDVI. Runoff and groundwater stability are critical factors for oasis restoration and sustainability [48]. These cases demonstrate that scientifically managed water allocations can effectively support the long-term stability of riparian forests, aligning with the conservation strategies proposed in this study. Long-term monitoring of *P. euphratica* stands, particularly in response to climate change and changing land use practices, will be essential for understanding the dynamic interactions between abiotic factors and tree physiology. Further research should explore the thresholds at which groundwater and soil salinity become detrimental to tree growth and how these factors interact with other environmental stressors. This will enable more effective conservation and management practices to safeguard *P. euphratica* populations and the ecosystem services they provide. To effectively mitigate degradation and protect *Populus euphratica* forests, this study recommends implementing targeted water diversion measures in *P. euphratica* distribution areas located farther from the river channel in the lower reaches of the Tarim River. These measures aim to enhance the restoration and regeneration of *P. euphratica* forests by improving water availability in these ecologically vulnerable regions.

5. Conclusions

The results of this study highlight substantial spatial variations in the structural characteristics and density of *Populus euphratica* trees along different transects of the Tarim River. In the upper reaches, tree density is higher, and the trees exhibit healthier growth, as indicated by greater H and DBH. In contrast, the middle and lower reaches show a clear decline in growth parameters, with reduced H, CD, and canopy cover, reflecting environmental stress and degradation. The age class distribution further emphasizes these differences, with the upper reaches supporting a balanced population of young and near-mature trees, while the lower reaches predominantly contain near-mature and mature trees, suggesting limited regeneration and an aging population.

Abiotic factors such as groundwater depth, soil salinity, annual precipitation, and soil moisture were identified as key drivers influencing the growth and structural development of *P. euphratica*. The findings underscore the critical role of water availability, particularly groundwater and soil moisture, in maintaining the health of riparian forests. These results contribute valuable insights into the resilience and health of desert riparian ecosystems and provide a basis for informed forest management and restoration strategies. Additionally, the application of TLS in this study demonstrates its potential for broader use in arid and semi-arid ecosystems. Beyond *P. euphratica* forests, TLS can provide high-precision structural assessments for other riparian and desert tree/shrub species, such as Tamarix, Haloxylon, and Salix, facilitating long-term monitoring and ecological modeling in water-limited environments. This research is important because it provides high-precision structural assessments of *P. euphratica* forests using TLS and multivariate analyses, enabling a more detailed understanding of the impact of abiotic factors on riparian ecosystems. The novel integration of PCA and RDA offers new insights into the hydrological and soil constraints affecting forest structure, highlighting key limiting factors for tree growth and regeneration.

Future research should focus on long-term monitoring of *P. euphratica* stands to assess the impacts of climate change and hydrological alterations on tree growth and regeneration dynamics. Additionally, further investigations into the thresholds of groundwater and salinity stress, as well as the potential for adaptive responses under extreme environmental conditions, are crucial to developing effective conservation strategies for this keystone species.

Author Contributions: A.A. (Alfidar Arkin) and A.Y.: Conceived the research ideas, designed the methodological framework, and wrote the manuscript's first draft; Ü.H. and A.Y.: Conceptualization, Supervision, Funding acquisition, Writing—review and editing; A.A. (Abdulla Abliz), A.T., A.A. (Ailiya Ainiwaer) and M.M.: Collected the field data, Validation, Visualization. All authors have read and agreed to the published version of the manuscript.

Funding: This study was supported by the Third Xinjiang Scientific Expedition and Research Program of the Ministry of Science and Technology of China [2022xjkk0300], the National Natural Science Foundation of China [32260285], the Postdoctoral Fellowship Program of CPSF [GZC20230067], and the China Postdoctoral Science Foundation [2024M750066].

Data Availability Statement: Data will be made available on request.

Acknowledgments: We thank Aishajiang Aili (Xinjiang Institute of Ecology and Geography, CAS) for the language polishing and improvement of this manuscript. Special thanks to Xinjiang LiDAR Applied Engineering Technology Center for renting the Riegl VZ-1000 TLS equipment. We also would like to express our gratitude to the editors and reviewers for their helpful comments and careful revision of this manuscript.

Conflicts of Interest: The authors declare no conflicts of interest.

References

1. Wang, S.J.; Chen, B.; Li, H. *Euphrates Poplar Forest*; China Environmental Science Press: Beijing, China, 1995.
2. Monda, Y.; Miki, N.; Yoshikawa, K. Stand structure and regeneration of *Populus euphratica* forest in the lower reaches of the Heihe River, NW China. *Landsc. Ecol. Eng.* **2008**, *4*, 115–124. [[CrossRef](#)]
3. Thomas, F.; Lang, P. Growth and water relations of riparian poplar forests under pressure in Central Asia's Tarim River Basin. *River Res. Appl.* **2020**, *37*, 233–240. [[CrossRef](#)]
4. Lang, P.; Ahlborn, J.; Schäfer, P.; Wommelsdorf, T.; Jeschke, M.; Zhang, X.; Thomas, F.M. Growth and water use of *Populus euphratica* trees and stands with different water supply along the Tarim River, NW China. *For. Ecol. Manag.* **2016**, *380*, 139–148. [[CrossRef](#)]
5. Yan, P.; He, G.; Wang, G. Spatial-temporal analysis of the changes in *Populus euphratica* distribution in the Tarim National Nature Reserve over the past 60 years. *Int. J. Appl. Earth Obs. Geoinf.* **2022**, *113*, 103000. [[CrossRef](#)]
6. Ndayambaza, B.; Si, J.; Deng, Y.; Jia, B.; He, X.; Zhou, D.; Wang, C.; Zhu, X.; Liu, Z.; Qin, J.; et al. The Euphrates Poplar Responses to Abiotic Stress and Its Unique Traits in Dry Regions of China (Xinjiang and Inner Mongolia): What Should We Know? *Genes* **2023**, *14*, 2213. [[CrossRef](#)] [[PubMed](#)]
7. Halik, Ü.; Aishan, T.; Betz, F.; Kurban, A.; Aihemaitijiang, R. Effectiveness and challenges of ecological engineering for desert riparian forest restoration along China's largest inland river. *Ecol. Eng.* **2019**, *127*, 11–22. [[CrossRef](#)]
8. Zeng, F.; Yan, H.; Stefan, A. Leaf and whole tree adaptations to mild salinity in field grown *Populus euphratica*. *Tree Physiol.* **2020**, *29*, 1237–1246. [[CrossRef](#)]
9. Yang, X.; Zhang, X.; Wang, X.; Hao, Z.X.; Singh, P.V.; Hao, F.H. Correction: Propagation from meteorological drought to hydrological drought under the impact of human activities: A case study in northern China. *J. Hydrol.* **2019**, *579*, 124147. [[CrossRef](#)]
10. Xu, H.; Chen, Y. Analysis of the desertification in lower reaches of Tarim River by multi-regression model. *Arid Land Resour. Environ.* **2003**, *17*, 78–82. [[CrossRef](#)]
11. Westermann, J.; Zerbe, S.; Eckstein, D. Age structure and growth of degraded *Populus euphratica* floodplain forests in NW China and perspectives for their recovery. *Integr. Plant Biol.* **2008**, *50*, 536–546. [[CrossRef](#)] [[PubMed](#)]
12. Guo, X.; Li, J.; Zhang, J.; Wei, C.; Li, Z. Vegetation growth improvement inadequately represents the ecological restoration of the *Populus euphratica* forests in Xinjiang, China. *Ecol. Indic.* **2025**, *170*, 113086. [[CrossRef](#)]

13. Gebeyehu, G.; Soromessa, T.; Bekele, T.; Teketay, D. Species composition, stand structure, and regeneration status of tree species in dry Afromontane forests of Awi zone, Northwestern Ethiopia. *Ecosyst. Health Sustain.* **2019**, *5*, 199–215. [[CrossRef](#)]
14. Looney, C.E.; D'Amato, A.W.; Palik, B.J.; Fraver, S.; Kastendick, D.N. Size-growth relationship, tree spatial patterns, and tree-tree competition influence tree growth and stand complexity in a 160-year red pine chronosequence. *For. Ecol. Manag.* **2018**, *424*, 85–94. [[CrossRef](#)]
15. Paul, A.; Khan, M.L.; Das, A.K. Population structure and regeneration status of rhododendrons in temperate mixed broad-leaved forests of western Arunachal Pradesh, India. *Geol. Ecol. Landsc.* **2019**, *3*, 168–186. [[CrossRef](#)]
16. Wiegand, T.; Moloney, K.A. *Handbook of Spatial Point-Pattern Analysis in Ecology*; CRC Press: Boca Raton, FL, USA, 2014.
17. Forman, R.T.T.; Hahn, D. Spatial patterns of trees in a Caribbean semievergreen forest. *J. Ecol.* **1980**, *61*, 1267. [[CrossRef](#)]
18. Dessard, H.; Picard, N.; Pélissier, R.; Collinet-Vaurier, F. Spatial patterns of the most abundant tree species. In *Ecology and Management of Neotropical Rainforest*; Elsevier: Paris, France, 2004.
19. Eusemann, P.; Petzold, A.; Thevs, N.; Schnittler, M. Growth patterns and genetic structure of *Populus euphratica* Oliv. (Salicaceae) forests in NW China—Implications for conservation and management. *For. Ecol. Manag.* **2013**, *297*, 27–36. [[CrossRef](#)]
20. Kramp, K.; Schmitt, T.; Lang, P.; Dulamsuren, C. Clones or no clones: Genetic structure of riparian *Populus euphratica* forests in Central Asia. *J. Arid Land.* **2018**, *10*, 750–766. [[CrossRef](#)]
21. Miao, N.; Jiao, P.P.; Tao, W.J.; Li, M.; Li, Z.; Hu, B.; Moermond, T.C. Structural dynamics of *Populus euphratica* forests in different stages in the upper reaches of the Tarim River in China. *Sci. Rep.* **2020**, *10*, 3196. [[CrossRef](#)]
22. Liu, Y.; Zeng, Y.; Wang, P.; He, J.; Li, P.; Liang, Y. The spatial pattern of *Populus euphratica* competition based on competitive exclusion theory. *Front. Plant Sci.* **2024**, *15*, 1276489. [[CrossRef](#)] [[PubMed](#)]
23. Calders, K.; Origo, N.; Burt, A.; Disney, M.; Nightingale, J.; Raunonen, P.; Åkerblom, M.; Malhi, Y.; Lewis, P. Realistic forest stand reconstruction from terrestrial LiDAR for radiative transfer modelling. *Remote Sens.* **2018**, *10*, 933. [[CrossRef](#)]
24. Chen, S.L.; Feng, Z.K.; Chen, P.P.; Khan, T.U.; Lian, Y.N. Nondestructive estimation of the above-ground biomass of multiple tree species in boreal forests of China using terrestrial laser scanning. *Forests* **2019**, *10*, 936. [[CrossRef](#)]
25. Yusup, A.; Halik, Ü.; Abdulla, A.; Keyimu, M.; Aishan, T.; Abliz, A.; Dilixiati, B.; Wei, J.X. Correction: Trunk volume estimation of irregular shaped *Populus euphratica* riparian forest using TLS point cloud data and multivariate prediction models. *For. Ecosyst.* **2023**, *10*, 100082. [[CrossRef](#)]
26. Li, Y.; Chen, Y.; Ye, C.; Wang, F.; Sun, F.; Qin, J. Ecological response of water conveyance in the lower Tarim River for 20 years. *Arid Land Geogr.* **2021**, *44*, 700–707. [[CrossRef](#)]
27. Goldbergs, G.; Levick, S.R.; Lawes, M.; Edwards, A. Hierarchical integration of individual tree and area-based approaches for savanna biomass uncertainty estimation from airborne LiDAR. *Remote Sens. Environ.* **2018**, *205*, 141–150. [[CrossRef](#)]
28. Yépez-Rincón, F.D.; Luna-Mendoza, L.; Ramírez-Serrato, N.L.; Corona, H.A.; Ferrino, A.L. Assessing vertical structure of an endemic forest in succession using terrestrial laser scanning (TLS). Case study: Guadalupe Island. *Remote Sens. Environ.* **2024**, *263*, 112563. [[CrossRef](#)]
29. O'Sullivan, H.; Raunonen, P.; Kaitaniemi, P.; Perttunen, J.; Sievänen, R. Integrating terrestrial laser scanning with functional-structural plant models to investigate ecological and evolutionary processes of forest communities. *Ann. Bot.* **2021**, *128*, 663–684. [[CrossRef](#)] [[PubMed](#)]
30. Wang, H.; Li, J.; Van de Voorde, T.; Zhou, C.; De Maeyer, P.; Ma, Y.; Shen, Z. Individual *Populus euphratica* tree detection in sparse desert forests based on constrained 2-D bin packing. *IEEE Trans. Geosci. Remote Sens.* **2024**, *62*, 1–19. [[CrossRef](#)]
31. Aishan, T.; Jiang, W.; Cheng, Q.; Halik, Ü.; Betz, F.; Yusup, A. Quantitative diagnosis of internal wood damage in living trees and its relationship with soil physicochemical properties: The case of an endangered desert riparian forest in Xinjiang, NW China. *For. Ecol. Manag.* **2024**, *561*, 121880. [[CrossRef](#)]
32. Crowther, T.W.; Glick, H.B.; Covey, K.R.; Bettigole, C.; Maynard, D.S.; Thomas, S.M.; Smith, J.R.; Hintler, G.; Duguid, M.C.; Amatulli, G.; et al. Mapping tree density at a global scale. *Nature* **2016**, *525*, 201–205. [[CrossRef](#)]
33. Valjarević, A.; Djekić, T.; Stevanović, V.; Ivanović, R.; Jandžiković, B. GIS numerical and remote sensing analyses of forest changes in the Toplica region for the period of 1953–2013. *Appl. Geogr.* **2018**, *92*, 131–139. [[CrossRef](#)]
34. Richardson, J.; Björheden, R. Estimating biomass of individual pine trees using airborne LiDAR. *Biomass Bioenergy* **2009**, *31*, 646–655. [[CrossRef](#)]
35. Liu, R.; Jiang, Y.; Chang, B.; Li, J.; Rong, C.; Liang, S.; Yang, R.; Liu, X.; Zeng, H.; Su, X.; et al. Interspecific associations and correlations among the main woody plants in a *Pterocarya stenoptera* community in a riparian zone of Lijiang River, Guilin, Southwest China. *Acta Ecol. Sin.* **2018**, *8*, 6881–6893. [[CrossRef](#)]
36. Ter Braak, C.J.F.; Šmilauer, P. *Canoco Reference Manual and User's Guide: Software for Ordination (Version 5.0)*; Microcomputer Power: Ithaca, NY, USA, 2012.
37. Han, L.; Wang, J.; Wang, H.; Niu, J.; Yu, J. Niche and spatial distribution pattern analysis of the main populations of the Tarim Desert-Oasis Ecotone. *Plant Sci. J.* **2016**, *34*, 352–360. [[CrossRef](#)]

38. Li, Q.; Feng, Q.; Zhai, L. Study of the height growth dynamic based on tree-ring data in *Populus euphratica* from the lower reach of the Heihe River, China. *Dendrochronologia* **2010**, *28*, 53–59. [[CrossRef](#)]
39. Ling, H.B.; Zhang, P.; Xu, H.L.; Zhao, X.F. How to regenerate and protect desert riparian *Populus euphratica* forest in arid areas. *Sci. Rep.* **2015**, *5*, 15418. [[CrossRef](#)] [[PubMed](#)]
40. Han, L.; Xi, L.Q.; Wang, J.Q.; Wang, H.Z.; Yu, Z.R. Life history characteristics and spatial distribution pattern of *Populus euphratica* population in the upper reaches of the Tarim River. *Acta Ecol. Sin.* **2013**, *33*, 6181–6190. [[CrossRef](#)]
41. Xu, M.; Chen, Y.; Liu, J.; Wang, D.; Liu, Y. The distribution pattern dynamics of *Populus euphratica* are influenced by hydrology in the middle reaches of the Tarim River. *Acta Ecol. Sin.* **2016**, *36*, 2646–2655.
42. Wu, J.X.; Zi, X.M.; Junxia, W.; Ximing, Z.; Chaozhou, D.; Guojun, L. Structure and dynamics of *Populus euphratica* population along Tarim River. *Pak. J. Bot.* **2012**, *44*, 1651–1656. [[CrossRef](#)]
43. Gärtner, P.; Förster, M.; Kurban, A.; Kleinschmit, B. Object based change detection of Central Asian Tugai vegetation with very high spatial resolution satellite imagery. *Int. J. Appl. Earth Obs. Geoinf.* **2014**, *31*, 110–121. [[CrossRef](#)]
44. Kath, J.; Reardon-Smith, K.; Le Brocq, A.F.; Dyer, F.J.; Dafny, E.; Fritz, L.; Batterham, M. Groundwater decline and tree change in floodplain landscapes: Identifying non-linear threshold responses in canopy condition. *Glob. Ecol. Conserv.* **2014**, *2*, 148–160. [[CrossRef](#)]
45. Ling, H.B.; Guo, B.; Xu, H.L.; Fu, J.Y. Configuration of water resources for a typical river basin in an arid region of China based on the ecological water requirements (EWRs) of desert riparian vegetation. *Glob. Planet Change* **2014**, *122*, 292–304. [[CrossRef](#)]
46. Chen, Y.; Li, W.; Zhou, H.; Chen, Y.; Hao, X.; Fu, A.; Ma, J. Experimental study on water transport observations of desert riparian forests in the lower reaches of the Tarim River in China. *Int. Biometeorol.* **2017**, *61*, 1055–1062. [[CrossRef](#)] [[PubMed](#)]
47. Li, X.; Li, Y.; Zhang, G.; Wang, L.; Yoshikawa, K. Regeneration properties of a *Populus euphratica* riparian forest located in the vicinity of the Ejina Oasis, Inner Mongolia, China. *Landsc. Ecol. Eng.* **2017**, *13*, 71–79. [[CrossRef](#)]
48. Wang, C.; Zhang, Y.; Zhao, W. Ecological hydrological restoration effects of ecological water conveyance in the lower reaches of the Heihe River and Ejina Oasis over the past two decades. *J. Ecol.* **2022**, *41*, 2180–2187. [[CrossRef](#)]

Disclaimer/Publisher’s Note: The statements, opinions and data contained in all publications are solely those of the individual author(s) and contributor(s) and not of MDPI and/or the editor(s). MDPI and/or the editor(s) disclaim responsibility for any injury to people or property resulting from any ideas, methods, instructions or products referred to in the content.